Proceedings of the 28th IEEE
EMBS Annual International Conference
New York City, USA, Aug 30-Sept 3, 2006

Parametric 3D Hip Joint Segmentation for the Diagnosis of Developmental Dysplasia

Rodrigo de Luis-García and Carlos Alberola-López

Abstract— **In this paper, we present a segmentation method for the hip joint from 3D ultrasound data. The proposed approach starts from a well-known energy formulation of the segmentation problem, and employs the extended local structure tensor as image feature in order to incorporate gray level and texture information in a common framework. Using the Kullback-Leibler distance as an intrinsic dissimilarity measure, the energy minimization is performed by estimating the optimal parameters of the shpere and paraboloid that best approximate the femoral head and acetabulum, respectively. A 2D level set segmentation of the iliac bone and an easy user interaction step allow for the introduction of the necessary constraints to make the energy minimization feasible.**
Experimental results over several data volumes show this approach to be capable of successfully approximating the anatomy of the hip joint by simple geometrical surfaces.

I. INTRODUCTION

The Developmental Dysplasia of the Hip (DDH) is a common congenital skeletal desease in newborns. It is characterized by an abnormal relation between the femoral head and the acetabulum. The importance of this pathology ranges from the dysplasia alone to the potential partial and complete dislocation of the hip. Moreover, DDH can develop with growth and severely alter the development of the articulation [1], [2], [3].

As early diagnosis of DDH is essential for a successful treatment, routine clinical screening of the newborns was introduced in the 50s [2]. Radiographic and ultrasound screening were incorporated later. While several examination techniques have been developed for ultrasound, Graf's method [4], [5] is the most established one.

Starting from a 2D ultrasound image of the hip joint taken in a defined plane, Graf's method is based on the assessment of the femoral head coverage by geometric measures. Specifically, the "bone angle" (α) and the "cartilage" angle (β) are quantified, as seen in Figure 1 (a).

Despite its widespread use, several objections have been made in the literature about Graf's technique. First, there is much debate about the value of the method, as it leads to difficulties in assessing the posterior coverage of the femoral head [3]. This problem is related to the monoplanar nature of this method, while DDH is a three-dimensional problem. Second, there is serious doubt about the inter-observer agreement when applying this technique [6]. These drawbacks, toghether with the Graf's method being a tedious and time consuming task, make the development of a computer aided diagnosis procedure for DDH a desirable goal.

Some effort has been done in the literature related to the use of 2D and 3D ultrasound data for the analysis of DDH. In [11], the femoral head and the acetabulum were segmented from 2D ultrasound images by applying anatomical prior knowledge to create shape priors which guide the segmentation process, performed in a level set environment. Even though these shape priors are necessary to perform the segmentation because of the lack of clear anatomical structures, they severely restrict the flexibility of the method. Therefore, it has difficulties to adapt to the high variability present in the hip joint ultrasound images. Besides, being a 2D technique, it does not take advantage of the benefits of 3D ultrasound screening of the hip. Although its use is far from being widespread in clinical practice, the use of 3D ultrasound is rapidly growing and might provide certain advantages over 2D screening [7]. In [8], [9], [10], effort was made on the determination and visualization of the femoral head from 3D ultrasound images.

In this paper, we present an automatic algorithm to segment the femoral head and the acetabulum by adjusting a sphere and a paraboloid. This way, the relative positions and parameters of these geometrical surfaces can be employed to perform the diagnosis of the DDH, and compared to the 2D geometrical measures used in Graf's method.

In order to obtain the optimal parameters of these geometrical surfaces, an appropriate energy functional is defined and minimized that takes into account both the gray level and texture information in the image. This energy term is based on the Geodesic Active Regions model [12] where, starting from a Bayesian formulation, a partition is created that is optimal according to the expected region properties. Instead of evolving a curve in a level set framework, the parameters of geometrical surfaces are optimized. This approach is very related to the introduction of shape constraints in a level set segmentation process, which has been successfully applied for medical images segmentation in the literature [13], [14]. As both gray level and texture information are of importance to perform the segmentation, the extended local structure tensor is employed as image feature [15]. Besides, as the Kullback-Leibler distance is applied as an intrinsic tensor dissimilarity measure, the energy term can be directly defined in the tensor domain.

The proposed method was applied on real 3D ultrasound volumes which were created from 2D images using a freehand 3D ultrasound reconstruction [16], [17] technique. Results

Rodrigo de Luis-García is with the Laboratorio de Procesado de Imagen, ETSI Telecomunicación University of Valladolid, 47011 Valladolid, Spain rodlui@tel.uva.es

Carlos Alberola-López is with the Laboratorio de Procesado de Imagen, ETSI Telecomunicación University of Valladolid, 47011 Valladolid, Spain caralb@tel.uva.es

1-4244-0033-3/06/$20.00 ©2006 IEEE.

show that the segmentation approach achieves good results and can help in the diagnosis of DDH.

The remainder of the paper is organized as follows: in the next section, we explain the theoretical foundations of the proposed segmentation method and describe the segmentation algorithm. In Section III, experimental results on real images are shown and discussed. Finally, conclusions and future work directions are presented.

II. METHODS

A. Local Structure Tensor

For a 3D scalar image I, the local structure tensor (LST) is defined as follows [18], [19], [20]:

$$J_\rho = K_\rho * (\nabla I \nabla I^T) = \begin{pmatrix} K_\rho * I_x^2 & K_\rho * I_x I_y & K_\rho * I_x I_z \\ K_\rho * I_x I_y & K_\rho * I_y^2 & K_\rho * I_y I_z \\ K_\rho * I_x I_z & K_\rho * I_y I_z & K_\rho * I_z^2 \end{pmatrix} \quad (1)$$

where K_ρ is a Gaussian kernel with standard deviation ρ, and subscripts denote partial derivatives.

Alternatively to the Gaussian smoothing, nonlinear diffusion can be applied to the LST as proposed by Brox and Weickert [21], [22] in order to avoid the dislocation of edges the Gaussian kernel can cause. For vector-valued data, the diffusion equation becomes:

$$\partial_t u_i = \text{div}\left(g\left(\sum_{k=1}^{N} |\nabla u_k|^2 \right) \nabla u_i \right) \quad \forall i \quad (2)$$

where u_i is an evolving vector channel, and N is the total number of vector channels.

The nonlinear local structure tensor (NLST) can be obtained by applying Eq. 2 with initial conditions $\mathbf{u} = [\, I_x^2 \quad I_y^2 \quad I_z^2 \quad I_x I_y \quad I_x I_z \quad I_y I_z \,]^T$. In practice, however, the original image is added as an extra channel because it can provide valuable information, yielding $\mathbf{u} = [\, I_x^2 \quad I_y^2 \quad I_z^2 \quad I_x I_y \quad I_x I_z \quad I_y I_z \quad I \,]^T$.

The described LST does not include any kind of gray level information, and thus it is not adequate as a unique image feature when the gray level information is also of importance. Thus, it is possible to incorporate this valuable information without losing the nice properties of the LST by using the *extended structure tensor* (ELST) [15]. For a scalar image, the ELST is defined as follows:

$$\mathbf{T_E} = D\left(vv^T\right) = \begin{pmatrix} \hat{I_x^2} & \hat{I_x I_y} & \hat{I_x I_z} & \hat{I_x I} \\ \hat{I_x I_y} & \hat{I_y^2} & \hat{I_y I_z} & \hat{I_y I} \\ \hat{I_x I_z} & \hat{I_y I_z} & \hat{I_z^2} & \hat{I_z I} \\ \hat{I_x I} & \hat{I_y I} & \hat{I_z I} & \hat{I^2} \end{pmatrix} \quad (3)$$

where $v = [\, I_x \quad I_y \quad I_z \quad I \,]^T$. $D()$ denotes the smoothing process applied to the tensor components, such as the Gaussian filtering or the nonlinear diffusion (which is also denoted by the hat operator).

B. Segmentation in the Tensor Domain

Following the work in [12], the image segmentation can be found by maximizing the *a posteriori* partition probability $p(\mathcal{P}(\Omega)|I)$ given the image I, where $\mathcal{P}(\Omega) = \{\Omega_1, \Omega_2\}$ is the partition of the image domain Ω in two regions. If we assume that all partitions are equally probable, and if the pixels within each region are conditionally independent, the maximization of the *a posteriori* segmentation probability is equivalent to the minimization of the following energy term (see [12] for details):

$$\begin{aligned} E(\Omega_1, \Omega_2) = & - \int_{\Omega_1} \log p(I(\mathbf{x})|\Omega_1) d\mathbf{x} \\ & - \int_{\Omega_2} \log p(I(\mathbf{x})|\Omega_2) d\mathbf{x} \end{aligned} \quad (4)$$

Now, let us consider the tensor valued image containing, at each voxel, the ELST of the original image described in the preceeding section, $\mathbf{T}(\mathbf{x})$. As proposed in [23], [24], the symmetrized Kullback-Leibler distance is an intrinsic dissimilarity measure for SPD tensors, and can be thus employed for the LST or its variants[15]. It can be shown that the square root of the symmetrized Kullback-Leibler distance turns out to have a very simple form [23]:

$$d_t(\mathbf{T_1}, \mathbf{T_2}) = \sqrt{\frac{1}{2} tr(\mathbf{T_1}^{-1}\mathbf{T_2} + \mathbf{T_2}^{-1}\mathbf{T_1}) - n} \quad (5)$$

where $tr(\cdot)$ is the matrix trace, and n is the size of the tensors $\mathbf{T_1}$ and $\mathbf{T_2}$.

Now, instead of modeling the intensity distributions as in Eq. 4, it is possible to model the distributions of the KL distances to their mean values, $\mathbf{T_1}$ and $\mathbf{T_2}$, in their respective domains. If we denote by $p_{d,1}$ and $p_{d,2}$ the densities of the KL distances to the respective tensor mean values, the energy term will then become:

$$\begin{aligned} E(\Omega_1, \Omega_2) = & - \int_{\Omega_1} \log p_{d,1}(d(\mathbf{T}(\mathbf{x}), \mathbf{T_1})) d\mathbf{x} \\ & - \int_{\Omega_2} \log p_{d,2}(d(\mathbf{T}(\mathbf{x}), \mathbf{T_2})) d\mathbf{x} \end{aligned} \quad (6)$$

For mathematical convenience we assume that $p_{d,1}$ and $p_{d,2}$ are Gaussian of zero mean and variances σ_1^2 and σ_2^2.

For the minimization of the defined energy, an evolving curve was employed in a level set framework in [15]. In this case, however, the energy term will be minimized with respect to the parameters of two different geometrical surfaces i.e. a sphere and a paraboloid. The Gaussian parameters will be updated at each iteration using

$$\sigma_i^2 = \frac{1}{|\Omega_i|} \int_{\Omega_i} d^2(\mathbf{T}(\mathbf{x}), \mathbf{T_i}) d\mathbf{x} \quad (7)$$

C. Segmentation Algorithm

As seen before, the proposed segmentation algorithm is based on the estimation of the optimal parameters of a sphere and a paraboloid by minimizing an energy functional. A critical step, however, is the adoption of an initial guess for these parameters, as the minimization by gradient step is very likely to get stuck in local mimima if the initial parameters are too distant from the optimal ones. The proposed algorithm consists of the following main steps:

- Determination of the distal end of the iliac bone. For this purpose, 2D slices are extracted from the 3D volume,

and the iliac bone contour is located using a 2D level set segmentation that works minimizing the energy term shown in Eq. 6 [15], [11]. Once the iliac bone has been segmented (see Figure 1 (b)), the distal end can be easily located for each slice. Finally, the segmented iliac bones from each slice are compared in terms of their areas in order to find the slice that defines the standard plane as employed in Graf's examination method (this slice will be hereafter referred to as central slice). This way, the three coordinates of the iliac bone end are located, $\mathbf{P} = (P_x, P_y, P_z)$.

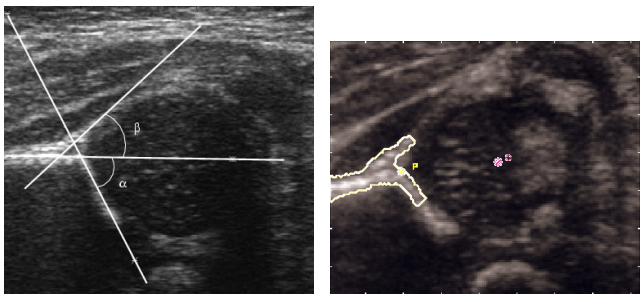

(a) (b)

Fig. 1. (a) 2D ultrasound image of the hip joint, toghether with the α and β angles employed in Graf's method for the diagnosis of DDH. (b) Automatically segmented iliac bone on central slice, and landmark $\mathbf{P}$.

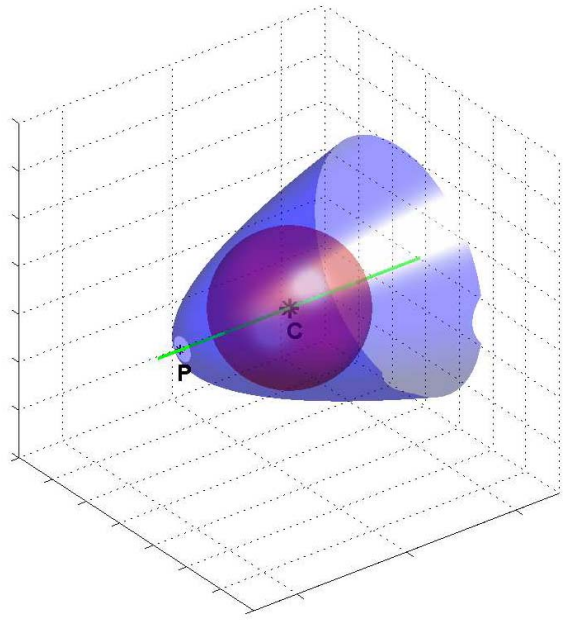

Fig. 2. Relative positions of the sphere segmenting the femoral head and the paraboloid segmenting the acetabulum.

- Determination of the initial center and radius for the sphere. Starting from point $\mathbf{P}$, intensity profiles from the central slice can be analyzed in order to obtain an initial guess for the center of the sphere, $\mathbf{C} = (C_x, C_y, C_z)$. Although using this procedure a fully automatic segmentation method will be completed, it is preferred to introduce a certain degree of user interaction in order to achieve the level of robustness required for a clinical application. In our case, the user is asked to locate the center of the femoral head in the central slice.
- Estimation of the optimal sphere using energy minimization. Starting from the initial parameters, $\mathbf{X_0} = (C_x, C_y, C_z, R)$, the energy functional in Eq. 6 is minimized in order to find the size and position of the sphere that best represents the femoral head. The position of point $\mathbf{P}$ is employed to impose an adittional contraint on the energy minimization process that prevents the sphere from growing beyond that point.
- Estimation of the optimal paraboloid. The acetabulum, the anatomical structure that embraces the femoral head, will be approximated by a paraboloid, a geometrical surface specified by the Cartesian equation $z = b(x^2 + y^2)$. Point $\mathbf{P}$ will be considered as the vertex of the paraboloid, and the line connecting $\mathbf{P}$ and $\mathbf{C}$ will be the axis. The described situation is graphically depicted in Figure 2. If we denote by u the position along this axis, the distance from any point $\mathbf{x}$ in the paraboloid can be also given, parametrically, by

$$d(\mathbf{x}, u) = a\sqrt{(u)} \tag{8}$$

Therefore, the only parameter that needs to be optimized for the paraboloid is parameter a in Eq. 8. Again, the energy term in Eq. 6 is minimized to obtain the optimal paraboloid to fit the acetabulum. An additional constraint is imposed so that the paraboloid is always outside the femoral head's sphere, as it is the case in the anatomy.

III. EXPERIMENTAL RESULTS

The 3D segmentation method proposed in this paper was tested on a set of 7 data volumes taken from four different newborns' hips. Freehand ultrasound reconstruction from 2D data was performed using a software module working over 3D Slicer [25], [26].

Starting from the reconstructed volumes, point $\mathbf{P}$ was successfully located in all cases. In Figure 1 (b), an example of the segmented iliac bone, toghether with point $\mathbf{P}$ and the user-specified sphere center, $\mathbf{C}$, are shown.

Following the segmentation algorithm described in the preceeding section, the approximated femoral head and acetabulum are obtained. In Figure 3, the intersection of the final sphere and paraboloid in the central slice are represented for two different cases.

The results obtained over our data set indicate that the estimated sphere and paraboloid adjust well to the femoral head and acetabulum. Starting from these geometrical surfaces, measures relating their positions and relative sizes can be extracted in order to develop a 3D procedure for the diagnosis of DDH.

Even though the obtained results are promising, some drawbacks have been encountered. First, the 3D freehand reconstruction employed to build the data volumes can cause

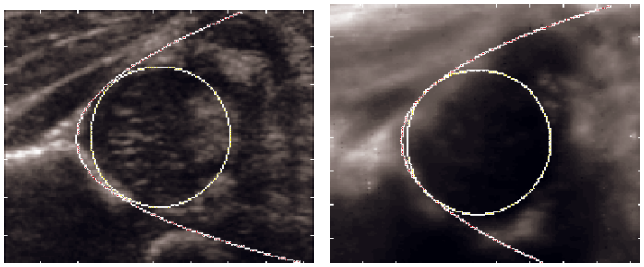

Fig. 3. 2D representation on the central slice of the segmenting sphere and paraboloid, for two different US volumes.

severe distortions in the data if any movement occurs during the exploration. This problem is expected to be solved with the use of intrinsic 3D ultrasound equipment. Second, in some cases the approximating paraboloid does not accurately fit the acetabulum in all regions, as this structure can present a very variable appearance. To solve this, a more complex geometrical surface might be needed to approximate the acetabulum.

IV. CONCLUSIONS AND FUTURE WORK

A parametric method for the segmentation of the femoral head and acetabulum from 3D ultrasound data has been presented. The problem is formulated in an energy minimization framework, and a set of parameters is optimized in order to find the sphere and the paraboloid that best fit the anatomical structures. Previously, a 2D segmentation process and a simple user interaction step are used so as to place two anatomically relevant landmarks that guide the segmentation. The proposed approach was tested over several US volumes, achieving promising results. Besides improving the robustness of the proposed algorithm and ensuring the adequacy of the aproximating surfaces, future work will focus on the study of the obtained 3D geometrical features in order to perform the diagnosis of DDH.

V. ACKNOWLEDGMENTS

The authors acknowledge the Comision Interministerial de Ciencia y Tecnologa, Spain, for research grant TEC2004-06647-C03-01, the Fondo de Investigaciones Sanitarias for grant PI-041483 and the Junta de Castilla y Leon for grant VA075A05; the European Commission is also acknowledged for the funds associated to the Network of Excellence SIMILAR (FP6-507609).

REFERENCES

[1] N. M. P. Clarke, "Congenital dislocation of the hip," *Current Orthopaedics*, vol. 18, pp. 256–261, 2004.

[2] P. Tomá, Maura Valle, U. Rossi, and G. Marré Brunenghi, "Paediatric hip-ultrasound screening for developmental dysplasia of the hip: a review," *European Journal of Ultrasound*, vol. 14, pp. 45–55, 2001.

[3] H. Gomes, T. Ouedraogo, C. Avisse, A. Lallemand and P. Bakhache, "Neonatal hip: from anatomy to cost-effective sonography, " *Pediatric Radiology*, vol. 8, pp. 1030–1039, 1998.

[4] R. Graf, "The diagnosis of congenital hip dislocation by the ultrasound compound treatment," *Archives of Orthopaedic and Trauma Surgery*, vol. 97, pp. 117–133, 1980.

[5] R. Graf, "Classification of hip-joint dysplasia by means of sonography," *Archives of Orthopaedic and Trauma Surgery*, vol. 102, no. 4, pp. 248–255, 1984.

[6] E. A. Simon, M. Buerge, R. Glaab, M. Roos, and G Kohler, "Inter-observer agreement of ultrasonographic measurement of alpha and beta angles and the final type classification based on the graf method," *Swiss Medical Weekly*, vol. 134, pp. 671–677, 2004.

[7] E. O. Gerscovich, A. Greenspan, M. S. Cronan, L. A. Karol, and J. P. McGahan, "Three-dimensional sonographic evaluation of developmental dysplasia of the hip: Preliminary findings," *Radiology*, vol. 190, pp. 407–410, 1994.

[8] H. M. Overhoff, D. Lazovic, J. Franke, and U. von Jan, "Automatic determination of the newborn's fermoral head from three-dimensional ultrasound image data," in *Proc. of the CVRMed-MRCAS'97, volume 1205 of Lecture Notes in Computer Science*, New York, USA, 1997, pp. 547–556.

[9] H. M. Overhoff, D. Lazovic, U. von Jan, and J. Franke, "Computer-based determination of the newborn's femoral head coverage using three-dimensional ultrasound scans," in *Proc. of the MICCAI'98, volume 1496 of Lecture Notes in Computer Science*, Cambridge, MA, USA, 1998, pp. 1024–1031.

[10] H. M. Overhoff, D. Lazovic, and U von Jan, "Visualization of the newborn's hip joint using 3-d ultrasound and automatic image processing," in *Proc. of SPIE Medical Imaging 1999*, 1999, pp. 1388–1395.

[11] R. de Luis-García and C. Alberola-López, "Hip Joint Segmentation for the Diagnosis of Developmental Dysplasia of the Hip Using Dynamic Shape Priors, " WSEAS Transactions on Signal Processing, " num. 3, vol. 1, pp. 432–438, 2005.

[12] Nikos Paragios and Rachid Deriche, "Geodesic active regions: A new framework to deal with frame partition problems in computer vision," *Journal of Visual Communication and Image Representation*, vol. 13, pp. 249–268, 2002.

[13] A. Tsai, A. Yezzi, W. Wells, C. Tempany, D. Tucker, A. Fan, W. E. Grimson, and A. Willsky, "A shape-based approach to the segmentation of medical imagery using level sets," *IEEE Transactions on Medical Imaging*, vol. 22, no. 2, pp. 137–154, feb 2003.

[14] J. Xie, H. Tsui, and W. Wai Man Lam, "Shape prior based segmentation for organ deformation correction," in *Proc. of the 2004 International Conference on Image Processing (ICIP)*, Singapore, 2004, pp. 2575–2578.

[15] R. de Luis-García, R. Deriche, M. Rousson, and C. Alberola-López, "Tensor processing for texture and colour segmentation," in *Proc. of the SCIA'05, volume 3540 of Lecture Notes in Computer Science*, New York, USA, 2005, pp. 1117–1127.

[16] R. W. Prager, A. H. Gee and L. Berman, "Stradx: real-time acquisition and visualisation of freehand 3D ultrasound," Cambridge University Department of Engineering, Tech. Rep., april 1998.

[17] R. W. Prager, R. Rohling, A. H. Gee and L. Berman, "Automatic calibration for 3-D free-hand ultradound," Cambridge University Department of Engineering, Tech. Rep., sept. 1997.

[18] W. Foerstner and E. Gulch, "A fast operator for detection and precise location of distinct points, corners and centres of circular features", in: Intercomm. Conf. on Fast Proc. of Photogrammetric. Data, Interlaken, June 1987, pp. 281-305.

[19] J. Bigun, G. H. Grandlund, and J. Wiklund, "Multidimensional orientation estimation with applications to texture analysis and optical flow," *IEEE Trans. on PAMI*, 13(8): 775-790, 1991.

[20] J. Bigun, G. H. Grandlund "Optimal orientation detection of linear symmetry," *Proc. 1st IEEE ICCV, London, June 1987*

[21] T. Brox and J. Weickert, "Nonlinear matrix diffusion for optic flow estimation," in *Proc. of the 24th DAGM Symp. , vol. 2449 of LNCS*, Zurich, Switzerland, sep 2002, pp. 446–453.

[22] T. Brox, J. Weickert, B. Burgeth, P. Mrázek "Nonlinear structure tensors", Preprint No. 113, Department of Mathematics, Saarland University, Saarbrücken, Germany. Oct. 2004

[23] Z. Wang and B. C. Vemuri, "An affine invariant tensor dissimilarity measure and its applications to tensor-valued image segmentation," in *Proc. of the IEEE CVPR*, Washington DC, USA, 2004, pp. 228–233.

[24] Z. Wang and B. C.Vemuri, "Tensor field segmentation using region based active contour model," in *Proc. of the ECCV*, Prague, Czech Republic, may 2004.

[25] 3D Slicer, Medical Visualization and Processing Environment for Research, "*http://www.slicer.org*".

[26] A. Galindo, "Desarrollo de un módulo en 3D Slicer para la adquisición y reconstrucción de volúmenes ecográficos mediante la técnica de manos libres, " Master Thesis, ETSI de Telecomunicación, University of Valladolid, Spain, jan. 2006.